Interaction of Excited Lithium Atom with Molecular Hydrogen. I. Preliminary Potential Energy Surfaces in an OVC MCSCF Approximation

Kimiko MIZUTANI,* Yoshihiro KURIBARA, Kazuko HAYASHI, and Shiro MATSUMOTO

Department of Chemistry, College of Science and Engineering, Aoyama Gakuin University, Chitosedai, Setagaya-ku, Tokyo 157

(Received November 16, 1978)

Potential energy surfaces were computed for the Li–H_2 system of C_{2v} symmetry, which dissociates to a normal hydrogen molecule and a lithium atom either in its ground state or in the ^2P excited state, in order to get an idea of the quenching process of the atom by the molecule. The potential surfaces crossed in a line and two shallow minima appeared on the $^2B_2$ surface. Natural orbital analysis and electron density maps gave information on the charge transfer character of the interaction of the excited atom with the molecule.

Quenching of excited atoms by diatomics is of interest as a prototype of elementary processes involving crossovers between adiabatic potential energy surfaces, *e. g.*, the processes involving the conversion of electronic excitation energies to those of chemical bonds. The present work was undertaken with the view that detailed understanding of the representative case would be an essential step in the clarification of these attractive molecular phenomena.

Bauer and his coworkers[1] published detailed calculations of the quenching process. They described a scheme which could be adjusted to yield results in substantial agreement with experiments in certain important aspects; the gross features of the scheme appeared reasonable from general theoretical points of view. The method they used to construct potential curves, though, involved many arbitrary and *ad hoc* assumptions.

Krauss[2] seems to be the first who undertook to calculate directly the potential curves for the simplest system of the class —Li–H_2. His results contained many important conclusions about the features of the system, which are in agreement with those of the present more comprehensive calculations. A few published[3] and unpublished[4] calculations have been performed for the system since then. Unfortunately, although they used elaborate extended bases and configurational interactions, they were restricted to special geometries of the system. The general description of the processes which occur in the electronic environment when the components come to interact seems, as far as we know, to be undocumented to date.

MCSCF calculations using OVC approximation[5] seem to be one of the reliable means to compute at least qualitatively the electronic structures of simpler systems, when the nuclear geometry is varied. As is well known, however, MCSCF calculations often suffer convergence difficulties, especially when the geometry changes greatly. A number of procedures[6] have been reported to overcome these difficulties. Some earlier calculations in this work were done by a method of direct minimization of the energy functional,[6a] which showed excellent stabilities toward iterations. The convergence of the method was rather slow, however, and most of the later calculations were performed using the coupling operator method proposed by Hirao and Nakatsuji[7] and Carbo,[8] into which quadratic convergency was incorporated.

The present paper reports the preliminary potential energy surfaces of the lowest $^2A_1$ and $^2B_2$ states of the Li–H_2 system in the C_{2v} symmetry. These states seem to be appropriate in describing the quenching process of Li(^2P) by H_2. Some features of the electronic structure of the system at several representative points on the surfaces are given also. The surfaces cross in a line; somewhere around this crossing, non-adiabatic transitions will occur as the result of perturbations. Two shallow minima appear on the $^2B_2$ surface, which may lead to exciplex formation.

Preliminary calculations showed that the potential energy surfaces of two linearly arranged Li–H_2 systems, which correlated to the isolated Li(^2S)+H_2 and to the isolated Li(^2P)+H_2, did cross as in the case of C_{2v} geometry. The lowest point of the crosssection, however, had a much higher (*ca.* 50 kcal/mol) energy than the point for the isolated Li(^2P)+H_2 system. A process *via* such arrangements seems to be inefficient in the quenching of Li(^2P) compared with the process presented above (activation energy≈4 kcal/mol). The results for linear geometry and for the general C_s geometries will be reported later, together with more detailed calculations near the crossing region using extended basis sets.

Method of Calculation

Geometry was restricted to the C_{2v} symmetry shown in Fig. 1. The bases were minimal STO-3G functions, as suggested by Pople *et al.*[9] and full CI was

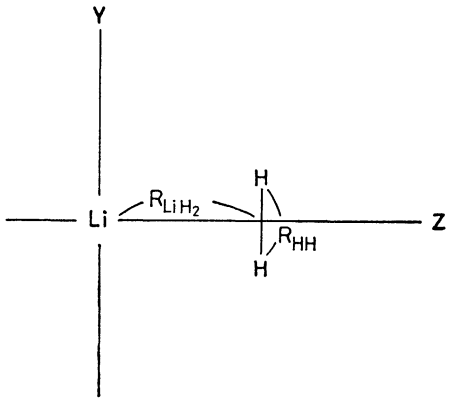

Fig. 1. Geometry of the system.

taken into account.

We take the OVC approximation[5] and express the electronic wavefunction Ψ as a linear combination of configurational wavefunctions differing only in the way the valence electrons occupy the molecular orbitals (MO):

$$\Psi = \sum_i A_i \Psi_{p_i r_i q_i}.$$

Of the five electrons of the system, two are assumed to occupy the core orbital and the remaining three are taken as valence electrons. In Ψ_{prq}, these electrons occupy p, r, and q valence orbitals with α, β, and α spin, respectively. When either p or q coincides with r, there is only one way of constructing a doublet configuration state function (CSF). If this is not the case, there arise two independent doublet CSF's of the same electronic configuration, and their forms are assumed to be

$$\Psi^{(1)}_{prq} = (D_{prq}+D_{rpq})/\sqrt{2}$$
$$\Psi^{(2)}_{prq} = (D_{prq}-D_{rpq}+2D_{pqr})/\sqrt{6},$$

where D_{prq} is the Slater determinant $(5!)^{-1/2}\,|\phi_1(1)\phi_{\bar{1}}(2)\phi_p(3)\phi_{\bar{r}}(4)\phi_q(5)|$. The energy expression for the OVC wave function is written:

$$E=\sum_{m,n}(h_{mn}+H^{core}_{mn})D^{core}_{mn}+\sum_{m,n}^{val.}\sum_{p,q}(C^{pq}h_{mn}+H^{pq}_{mn})b^p_m b^q_n,$$

where b^p_m are the expansion coefficients of the p-th orbital, h_{mn} are the matrix elements of the bare-nucleus Hamiltonian, and D^{core}_{mn} are the elements of the core density matrix $\sum_r^{core} b^r_m b^r_n$. H^{core}_{mn} and H^{pq}_{mn} are defined as

$$H^{core}_{mn} = h_{mn} + \sum_{k,l}\{D^{core}_{kl}+\sum_{p,q}^{val.}C^{pq}b^p_k b^q_l\}(2J_{mnkl}-K_{mnkl}),$$
$$H^{pq}_{mn} = C^{pq}\{h_{mn}+\sum_{k,l}D^{core}_{kl}(2J_{mnkl}-K_{mnkl})\} + \sum_{k,l}\sum_{r,s}^{val.}R^{pq}_{rs}b^r_k b^s_l J_{mnkl},$$

where J_{mnkl} and K_{mnkl} are the coulombic and the exchange repulsion integrals. C^{pq} and R^{pq}_{rs} are the coefficients of averaged occupancies of valence orbitals and have similar meanings to the terms $P^{(s)AO}_{1AB}$ and $P^{(s)AO}_{2ABCD}$ of Ref. 6a. In this special case, they are written as

$$R^{pq}_{rs} = 2\{\sum_{t(\neq r,s)}A_{tpr}A_{tqs}+\sum_{t(\neq p,q)}A_{prt}A_{qst}+\sum_t A_{ptr}A_{qts}\},$$
$$C^{pq} = \sum_t^{val.}R^{tt}_{pq}/2,$$

where A_{prq} are the expansion coefficients in $\Psi=\sum_{p,r,q}A_{prq}D_{prq}$. According to the formulation of Carbo,[8] every molecular orbital wavefunction ϕ^p is an eigenfunction of a coupling operator $\mathbf{R}$.

$$\mathbf{R}|\phi^p\rangle = |\phi^p\rangle\varepsilon^p \qquad (1)$$

When approximate orbital functions given by the last iteration are used as a temporary basis, the matrix elements of $\mathbf{R}$ are given as follows. For diagonal elements:

$$R_{rr} = \sum_i b^r_i F^r_i + \beta_r, \quad R_{vv} = \sum_{i,j}b^v_i H^{occ}_{ij}b^v_j + \beta_v$$

and for non-diagonal elements:

$$R_{rs} = \lambda_{rs}\sum_i(b^r_i F^s_i - b^s_i F^r_i), \quad R_{vr} = \sum_i b^v_i F^r_i,$$

$$R_{vv'} = \sum_{i,j}b^v_i H^{occ}_{ij}b^{v'}_j,$$

where $F^r_i=\sum_{s,j}H^{rs}_{ij}b^s_j$ (r,s: valence), $F^r_i=\sum_j H^{core}_{ij}b^r_j$ (r: core), and $\mathbf{H}^{occ}=1/2\sum_{p,q}^{occ}(\mathbf{H}^{pq}+\mathbf{H}^{qp})$. Superfixes r and s refer to occupied orbitals and v and v' refer to vacant orbitals. The value β_p is the level shift given to the MO p. The absolute values of the nondiagonal matrix element λ_{rs} were usually taken to be unity. At later stage of iteration using Eq. 1 alone, the convergence was often slow, and quadratic convergency was incorporated into the computing program along with the Newton-Raphson procedure, as done by Hunt, Goddard, and Dunning.[10] The resultant formulation appears to be similar to that given by Hinze.[6b]

Results and Discussion

Potential Energy Surface. The computed energies of the ground state ($^2A_1$) and the first excited state ($^2B_2$) are shown in the contour maps of Figs. 2 and 3, respectively, as functions of two distances R_{HH} and R_{LiH_2}. The first state dissociates to a normal lithium

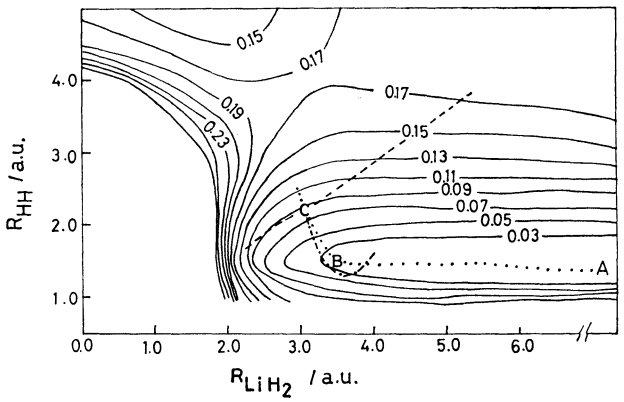

Fig. 2. Potential energy surface for $^2A_1$ ground state. R_{LiH_2} is the distance in bohrs from the Li nucleous to the midpoint of the line connecting the two hydrogens. R_{HH} is the distance between the hydrogens. The figures beside contours are energies in hartrees minus −8.47.

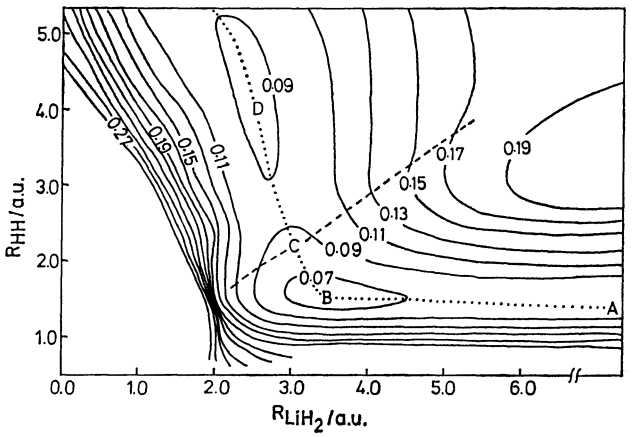

Fig. 3. Potential energy surface for the lowest $^2B_2$ state. The figures beside contours are energies in hartrees minus −8.47.

atom and a hydrogen molecule, while the latter is seen to dissociate to an excited lithium (^2P) atom and a hydrogen molecule in the ground state. The energy surface of the $^2B_2$ state is seen to have two minima, one at $R_{LiH_1}\approx3.5$ a.u., $R_{HH}\approx1.5$ a.u., and the other at $R_{LiH_1}\approx2.5$ a.u., $R_{HH}\approx4.0$ (a.u.). The calculated depth of the former was 9.5 kcal/mol, with respect to the isolated system of Li(^2P) and H_2 ($^1\Sigma_g$). The bottom of the latter was calculated to lie 6.2 kcal/mol above the isolated system, and to be separated by some potential barrier (see below). These minima might correspond to exciplexes, if any exist, between an excited Li atom and a hydrogen molecule. The general appearance of the $^2A_1$ surfaces is similar to that of the $^2B_2$ surface, but no minima appear in the lower-right valley, and the surface in Fig. 2 is more steeply ascending toward the upper-left region than is the $^2B_2$ surface in Fig. 3. The two potential surfaces intersect in a curve, which is shown by broken lines in Figs. 2 and 3.

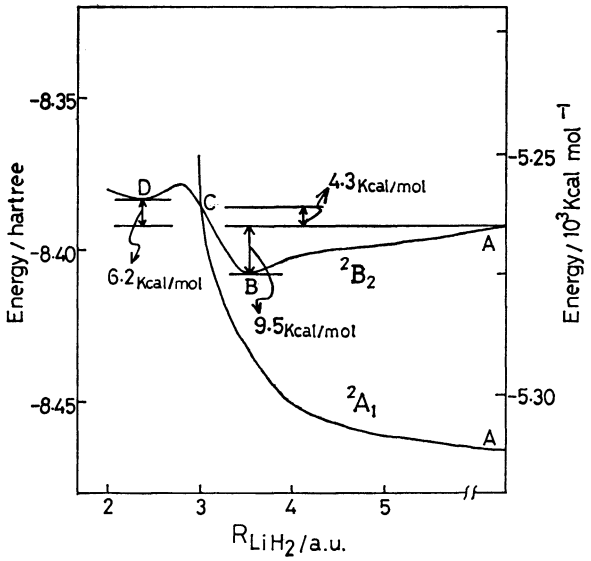

Fig. 4. Energies along minimum energy path.

On these potential surfaces, we might picture the quenching process of excited lithium atoms by hydrogen molecules through geometries close to C_{2v}. Starting from point A in Fig. 3, the path of energetically most favorable approach, *i.e.* the path of quasi-static approach, is shown by the dotted lines in Figs. 2 and 3, and the change of energy along the path is shown schematically in Fig. 4.** The crossing point of $^2A_1$ and $^2B_2$ curves in Fig. 4 is the point of lowest energy on the broken line of Fig. 3. The geometry was found to be $R_{HH}\approx3.0$ a.u. and $R_{LiH_1}\approx2.2$ (a.u.). Activation energy was 4.3 kcal/mol. Transitions at nearby geometries between the surfaces may become possible by contributions of vibrations of appropriate symmetry or by proper

** In actuality, the path would wander somewhat, as is shown partly by the chain line in Fig. 2, thus resulting in a vibrationally excited H_2 molecule. Some coupling of vibrational motion to the translational motion should also exist in the ascending path on the $^2B_2$ surface. To get actual reaction paths is, however, not in the scope of this paper.

TABLE 1. CI WAVE FUNCTIONS OF THE $^2B_2$ STATE AT FOUR TYPICAL GEOMETRIES: A, B, C, AND D, IN Fig. 3

CSF[a]	CI coefficient Geometry			
	A[b]	B[c]	C[d]	D[e]
$1a_1^2 2a_1^2 1b_2$	0.9937	0.9921	0.9823	0.9695
$1a_1^2 3a_1^2 1b_2$	0.0	−0.0320	−0.0422	−0.0685
$1a_1^2 1b_2 1b_1^2$	0.0	0.0023	0.0076	0.0231
$1a_1^2 1b_2 2b_2^2$	0.1121	0.1039	0.1137	0.0475
$1a_1^2 2b_2 1b_1^2$	0.0	0.0008	0.0031	−0.0036
$1a_1^2 2a_1^2 2b_2$	0.0	−0.0039	−0.0122	0.0183
$1a_1^2 3a_1^2 2b_2$	0.0	−0.0032	−0.0120	0.0227
$1a_1^2 4a_1^2 1b_2$	0.0	−0.0006	−0.0007	−0.0059
$1a_1^2 4a_1^2 2b_2$	0.0	0.0	−0.0003	0.0015
$1a_1^2 1b_2^2 2b_2$	0.0	0.0350	0.0924	−0.1227
$1a_1^2 2a_1 3a_1 1b_2$	0.0	−0.0230	−0.0129	−0.1667
$1a_1^2 2a_1 3a_1 1b_2$	0.0	0.0003	−0.0024	−0.0032
$1a_1^2 2a_1 3a_1 2b_2$	0.0	0.0444	−0.0937	0.0702
$1a_1^2 2a_1 3a_1 2b_2$	0.0	−0.0035	−0.0461	0.0602
$1a_1^2 2a_1 4a_1 1b_2$	0.0	0.0	−0.0001	−0.0003
$1a_1^2 2a_1 4a_1 1b_2$	0.0	0.0098	0.0164	0.0071
$1a_1^2 2a_1 4a_1 2b_2$	0.0	−0.0007	−0.0065	0.0139
$1a_1^2 2a_1 4a_1 2b_2$	0.0	0.0064	0.0048	0.0024
$1a_1^2 3a_1 4a_1 1b_2$	0.0	−0.0061	0.0033	0.0003
$1a_1^2 3a_1 4a_1 1b_2$	0.0	−0.0014	0.0010	−0.0006
$1a_1^2 3a_1 4a_1 2b_2$	0.0	−0.0001	−0.0011	0.0025
$1a_1^2 3a_1 4a_1 2b_2$	0.0	0.0004	−0.0019	0.0015

a) Configuration state function. The last twelve CSF's represent six pairs, the two members of each pair corresponding to two different spin states of same configuration. b) $R_{LiH_1}=100$ a.u., $R_{HH}=1.4$ a.u. c) $R_{LiH_1}=3.5$ a.u., $R_{HH}=1.5$ a.u. d) $R_{LiH_1}=3.02$ a.u., $R_{HH}=2.2$ a.u. e) $R_{LiH_1}=2.5$ a.u., $R_{HH}=4.0$ a.u.

TABLE 2. NATURAL ORBITALS CONSTITUTING CONFIGURATIONS IN TABLE 1

Molecular orbital	Basis function	Molecular orbital coefficient Geometry			
		A	B	C	D
ϕ_{1a_1}	$H_2\ 1\sigma_g$	0.0	−0.0122	0.0037	0.0005
	Li 1s	0.9950	0.9955	0.9950	0.9960
	Li 2s	0.0267	0.0268	0.0253	0.0212
	Li $2p_z$	0.0	0.0002	−0.0023	−0.0055
ϕ_{2a_1}	$H_2\ 1\sigma_g$	1.0	0.9578	0.8362	0.6164
	Li 1s	0.0	−0.0465	−0.0996	−0.1298
	Li 2s	0.0	0.0464	0.1614	0.4030
	Li $2p_z$	0.0	0.0486	0.1509	0.2488
ϕ_{3a_1}	$H_2\ 1\sigma_g$	0.0	−0.8300	1.1018	1.2298
	Li 1s	−0.1967	−0.1517	0.1253	0.1181
	Li 2s	0.9819	0.9657	−1.0672	−1.1571
	Li $2p_z$	−0.2542	0.8351	−0.8719	−0.6216
ϕ_{4a_1}	$H_2\ 1\sigma_g$	0.0	−0.2274	−0.2984	−0.4562
	Li 1s	−0.0517	0.1271	0.1265	0.0936
	Li 2s	0.2581	−0.5766	−0.5100	−0.2526
	Li $2p_z$	0.9671	0.8521	0.9099	1.0591
ϕ_{1b_2}	$H_2\ 1\sigma_u$	0.0	0.1260	0.3937	0.7666
	Li $2p_y$	1.0	0.9632	0.8030	0.3778
ϕ_{2b_2}	$H_2\ 1\sigma_u$	1.0	1.0204	0.9780	−0.8300
	Li $2p_y$	0.0	−0.3597	−0.6832	1.0648
ϕ_{1b_1}	Li $2p_x$	1.0	1.0	1.0	1.0

Table 3. CI wave functions of the $^2A_1$ ground state at four typical geometries: A, B, C, and D, in Fig. 2

CSF	CI coefficient Geometry			
	A	B	C	D
$1a_1^2 2a_1^2 3a_1$	0.9937	0.9921	0.9776	0.3540
$1a_1^2 2a_1^2 3a_1^2$	0.0	−0.0016	−0.0053	−0.0780
$1a_1^2 2a_1 1b_2^2$	0.0	0.0115	0.0249	0.8903
$1a_1^2 3a_1 1b_2^2$	0.1121	0.1185	0.2033	0.0525
$1a_1^2 2a_1 1b_1^2$	0.0	−0.1160	−0.0181	−0.0187
$1a_1^2 3a_1 1b_1^2$	0.0	0.0024	0.0052	0.0059
$1a_1^2 2a_1 4a_1^2$	0.0	0.0076	0.0088	−0.0169
$1a_1^2 3a_1 4a_1^2$	0.0	0.0254	0.0263	0.0040
$1a_1^2 2a_1 2b_2^2$	0.0	−0.0105	−0.0144	−0.1056
$1a_1^2 3a_1 2b_2^2$	0.0	0.0019	0.0037	0.0452
$1a_1^2 4a_1 1b_2^2$	0.0	−0.0005	−0.0016	0.0050
$1a_1^2 4a_1 2b_2^2$	0.0	0.0015	0.0021	0.0017
$1a_1^2 4a_1 1b_1^2$	0.0	0.0015	0.0021	−0.0005
$1a_1^2 2a_1^2 4a_1$	0.0	−0.0002	0.0001	−0.0076
$1a_1^2 3a_1^2 4a_1$	0.0	0.0091	0.0090	0.0020
$1a_1^2 2a_1 3a_1 4a_1$	0.0	0.0030	0.0026	−0.0035
$1a_1^2 2a_1 3a_1 4a_1$	0.0	0.0018	0.0015	−0.0058
$1a_1^2 2a_1 1b_2 2b_2$	0.0	−0.0197	−0.0298	−0.1716
$1a_1^2 2a_1 1b_2 2b_2$	0.0	−0.0042	−0.0073	0.1152
$1a_1^2 3a_1 1b_2 2b_2$	0.0	0.0001	0.0010	−0.0026
$1a_1^2 3a_1 1b_2 2b_2$	0.0	0.0001	0.0007	−0.1276
$1a_1^2 4a_1 1b_2 2b_2$	0.0	−0.0001	−0.0017	0.0095
$1a_1^2 4a_1 1b_2 2b_2$	0.0	0.0003	0.0007	−0.0115

Table 4. Natural orbitals constituting configurations in Table 3

Molecular orbital	Basis function	Molecular orbital coefficient Geometry			
		A	B	C	D
ϕ_{1a_1}	H_2 $1\sigma_g$	0.0	−0.0060	−0.0022	0.0050
	Li 1s	0.9952	0.9954	0.9957	0.9948
	Li 2s	0.0257	0.0262	0.0239	0.0253
	Li $2p_z$	0.0	0.0031	0.0011	−0.0017
ϕ_{2a_1}	H_2 $1\sigma_g$	1.0	0.9713	0.9033	0.7148
	Li 1s	0.0	−0.0512	−0.0864	−0.1383
	Li 2s	0.0	0.0295	0.0915	0.3538
	Li $2p_z$	0.0	0.0357	0.0988	0.1391
ϕ_{3a_1}	H_2 $1\sigma_g$	0.0	−0.1829	−0.1779	−0.7938
	Li 1s	−0.2024	−0.1820	−0.1683	−0.1512
	Li 2s	1.0152	0.9646	0.9236	1.1191
	Li $2p_z$	0.0	−0.3565	−0.4422	−0.0323
ϕ_{4a_1}	H_2 $1\sigma_g$	0.0	−0.8254	−1.0746	−0.9795
	Li 1s	0.0	−0.0760	−0.0661	0.0033
	Li 2s	0.0	0.5796	0.7509	0.4328
	Li $2p_z$	1.0	1.1391	1.1856	1.2448
ϕ_{1b_1}	H_2 $1\sigma_u$	1.0	1.0045	0.9958	0.7039
	Li $2p_y$	0.0	−0.0202	0.0129	0.4546
ϕ_{2b_1}	H_2 $1\sigma_u$	0.0	−0.2193	−0.3462	−0.8838
	Li $2p_y$	1.0	1.0279	1.0542	1.0344
ϕ_{1b_2}	Li $2p_x$	1.0	1.0	1.0	1.0

deformations from C_{2v} symmetry. Thus the way in which the electronic energy is converted to the vibrational and translational energies of the hydrogen molecule may easily be visualized.

Some Remarks on the Wave Function. Tables 1 and 2 show the computed $^2B_2$ wave functions as expressed by natural orbital expansions at four typical geometries on the dotted line in Fig. 3. Tables 3 and 4 show, for comparison, the corresponding $^2A_1$ wave functions at these geometries. As is seen in Table 1, the predominant CSF in the expansion of the $^2B_2$ wave function is always $\Psi_{2a_1 2a_1 1b_1}$. Table 2 shows that the orbitals ϕ_{2a_1} and ϕ_{1b_1} are always bonding in the sense that they pile up electron densities between the Li atom and the H_2 molecule. They are seen, however, to cause electrons to migrate in opposite directions. The occupation of ϕ_{1b_1} means more and more electron migrations from the Li $2p_y$ atomic orbital to the $1\sigma_u$ hydrogen molecular orbital, as we go down the series of geometries from A to D. The occupation of ϕ_{2a_1} means, on the contrary, electron migrations from the fully occupied $1\sigma_g$ hydrogen MO to the nearly sp hybridized Li 2s and $2p_z$ atomic orbitals, though the extent of charge migration is less remarkable than in the case of ϕ_{1b_1}.

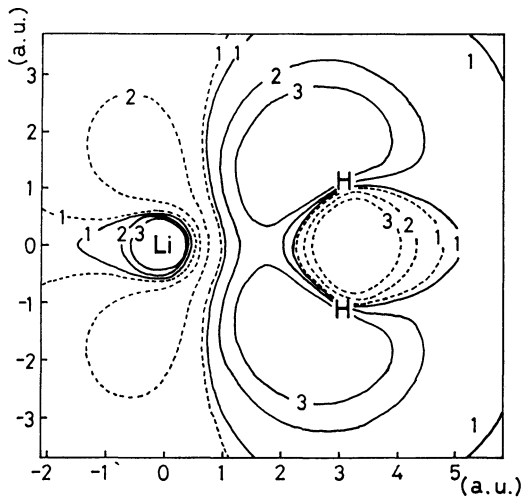

Fig. 5. Contour plots of total electron density of $^2B_2$ state at the geometry C in Fig. 3 minus the density of hypothetical $^2B_2$ state lacking in the interaction between Li and H_2. Full lines correspond to positive and broken lines to negative values of difference. The numbers 1, 2, 3 beside the contours indicate electron density change of 2.0×10^{-4}, 2.0×10^{-3}, 4.0×10^{-3} electrons/a.u.^{3}, respectively.

The predominant configuration in the $^2A_1$ state is $\Psi_{2a_1 2a_1 3a_1}$ for the geometries A, B, and C, but is $\Psi_{2a_1 1b_1 1b_1}$ for the geometry D. In the three former cases, double occupation of ϕ_{2a_1} effects a similar charge migration to that in the $^2B_2$ state and the occupation of ϕ_{3a_1} is seen to affect the charge migration only slightly. The net effect is that the electron transfer in the $^2A_1$ complex is in the opposite direction (from hydrogen toward lithium) to that in the $^2B_2$ complex. This may be important in the stabilization of the $^2B_2$ complex relative to the $^2A_1$ state. The situation at the C geometry is made more visual in Fig. 5, where the electron densities of the $^2B_2$ state minus the electron densities of a hypothetical system, in which the interactions between Li and H_2 have been artificially removed, are

plotted as contour lines: full-lines indicate an increase and dotted lines indicate a decrease in electron densities upon interaction. As noted above, the predominant configurations of the $^2A_1$ state at the D geometry has changed to $\Psi_{2a_1 1b_1 1b_1}$. In this case, the occupation of ϕ_{1b_1} also causes electrons to migrate from H_2 to Li, though the region of charge redistribution is different from that in the ϕ_{2a_1}. Fuller account of the analysis of the situation will be given in a succeeding paper.

The potential surfaces and electronic wave functions given here are preliminary in that the basis functions used are limited. It is hoped, however, that the results are at least qualitatively correct[4] and will be a useful starting point for more quantitative investigations. Work is going on to extend the bases to reach wave functions which could be used in a quantitative description of the non-adiabatic transitions in the interaction of excited atoms with molecules.

The authors wish to thank Dr. S. Iwata of the Institute of Physical and Chemical Research for his helpful discussions. They also express their gratitude to the Aoyama Gakuin Computing Center, where all computations were carried out on an IBM 370-138. Thanks are due to Miss J. Okamura, Miss J. Oga, Miss K. Yahata, and Mr. H. Miyoshi for their help in these computations.

References

1) E. Bauer, E. R. Fisher, and F. R. Gilmore, *J. Chem. Phys.*, **51**, 4173 (1969).
2) M. Krauss, *J. Res. Natl. Bur. Stand., Sect. A* **72**, 553 (1968).
3) P. J. A. Ruttink and J. H. van Lenthe, *Theor. Chim. Acta*, **44**, 97 (1977).
4) H. F. Schaefer III, "Method of Electronic Structure Theory," Plenum Pub. Corp., New York (1976), p. 51.
5) A. C. Wahl and G. Das, *Adv. Quant. Chem.*, **5**, 261 (1970); G. Das and A. C. Wahl, *J. Chem. Phys.*, **44**, 87 (1966); *ibid.*, **56** 3532 (1972).
6) a) S. Polezzo, *Theor. Chim. Acta*, **40**, 245 (1975); P. Fantucci and S. Polezzo, *ibid.*, **44**, 421 (1977); b) J. Hinze, *J. Chem. Phys.*, **59**, 6424 (1973); c) G. Das and A. C. Wahl, *ibid.*, **56** 1769 (1972).
7) K. Hirao and H. Nakatsuji, *J. Chem. Phys.*, **59**, 1457 (1973).
8) R. Carbo, R. Gallifa, and J. M. Riera, *Chem. Phys. Lett.*, **33**, 545 (1975).
9) W. J. Hehre, R. F. Stewart, and J. A. Pople, *J. Chem. Phys.*, **51**, 2657 (1969).
10) W. J. Hunt, W. A. Goddard, III, and T. H. Dunning, Jr., *Chem. Phys. Lett.*, **6**, 147 (1970).